

High bandwidth, high responsivity waveguide-coupled germanium p-i-n photodiode

Stefan Lischke,^{1,*} Dieter Knoll,¹ Christian Mai,¹ Lars Zimmermann,¹ Anna Peczek,¹ Marcel Kroh,¹ Andreas Trusch,¹ Edgar Krune,² Karsten Voigt,² and A. Mai¹

¹IHP, Im Technologiepark 25, 15236 Frankfurt (Oder), Germany

²Technical University Berlin, Institut für Hochfrequenz- und Halbleiter-Systemtechnologien, Einsteinufer 25, 10587 Berlin, Germany

*lischke@ihp-microelectronics.com

Abstract: A novel waveguide-coupled germanium p-i-n photodiode is demonstrated which combines high responsivity with very high -3 dB bandwidth at a medium dark current. Bandwidth values are 40 GHz at zero bias and more than 70 GHz at -1 V. Responsivity at 1.55 μm wavelength ranges from 0.84 A/W at zero bias to 1 A/W at -1 V. Room temperature dark current density at -1 V is about 1 A/cm². The high responsivity mainly results from the use of a new, low-loss contact scheme, which moreover also reduces the negative effect of photo carrier diffusion on bandwidth.

©2015 Optical Society of America

OCIS codes: (130.3120) Integrated optics devices; (160.6000) Semiconductor materials; (230.5160) Photodetectors.

References and links

1. G. Masini, S. Sahni, G. Capellini, J. Witzens, and C. Gunn, "High-speed near infrared optical receivers based on Ge waveguide photodetectors integrated in a CMOS process," *Adv. Opt. Technol.* **2008**, 196572 (2008).
2. C. T. DeRose, D. C. Trotter, W. A. Zortman, A. L. Starbuck, M. Fisher, M. R. Watts, and P. S. Davids, "Ultra compact 45 GHz CMOS compatible germanium waveguide photodiode with low dark current," *Opt. Express* **19**(25), 24897–24904 (2011).
3. J. Michel, J. Liu, and L. C. Kimerling, "High-performance Ge-on-Si photodetectors," *Nat. Photonics* **4**(8), 527–534 (2010).
4. S. Liao, N.-N. Feng, D. Feng, P. Dong, R. Shafiiha, C.-C. Kung, H. Liang, W. Qian, Y. Liu, J. Fong, J. E. Cunningham, Y. Luo, and M. Asghari, "36 GHz submicron silicon waveguide germanium photodetector," *Opt. Express* **19**(11), 10967–10972 (2011).
5. L. Vivien, J. Osmond, J.-M. Fédéli, D. Marris-Morini, P. Crozat, J.-F. Damlencourt, E. Cassan, Y. Lecunff, and S. Laval, "42 GHz p.i.n germanium photodetector integrated in a silicon-on-insulator waveguide," *Opt. Express* **17**(8), 6252–6257 (2009).
6. A. Novack, M. Gould, Y. Yang, Z. Xuan, M. Streshinsky, Y. Liu, G. Capellini, A. E. Lim, G.-Q. Lo, T. Baehr-Jones, and M. Hochberg, "Germanium photodetector with 60 GHz bandwidth using inductive gain peaking," *Opt. Express* **21**(23), 28387–28393 (2013).
7. L. Viro, L. Vivien, J.-M. Fédéli, Y. Bogumilowicz, J.-M. Hartmann, F. Boeuf, P. Crozat, D. Marris-Morini, and E. Cassan, "High-performance waveguide-integrated germanium PIN photodiodes for optical communication applications," *Photonics Research* **1**(3), 140–147 (2013).
8. L. Vivien, A. Polzer, D. Marris-Morini, J. Osmond, J. M. Hartmann, P. Crozat, E. Cassan, C. Kopp, H. Zimmermann, and J.-M. Fédéli, "Zero-bias 40Gbit/s germanium waveguide photodetector on silicon," *Opt. Express* **20**(2), 1096–1101 (2012).
9. D. Knoll, S. Lischke, L. Zimmermann, B. Heinemann, D. Micusik, P. Ostrovskyy, G. Winzer, M. Kroh, R. Barth, T. Grabolla, K. Schulz, M. Fraschke, M. Lisker, J. Drews, A. Trusch, A. Krüger, S. Marschmeyer, H. H. Richter, O. Fursenko, Y. Yamamoto, B. Wohlfeil, K. Petermann, A. Beling, Q. Zhou, and B. Tillack, "Monolithically integrated 25Gbit/sec receiver for 1.55 μm in photonic BiCMOS technology," in *Optical Fiber Communication Conference* (Optical Society of America, 2014), paper Th4C.4.
10. A. C. Berti and S. P. Baranowski, "Self-aligned cobalt silicide on MOS integrated circuits," US Patent, No. 5736461, April 7, 1998.
11. T. Canneaux, D. Mathiot, J.-P. Ponpon, and Y. Leroy, "Modeling of phosphorus diffusion in Ge accounting for a cubic dependence of the diffusivity with the electron concentration," *Thin Solid Films* **518**(9), 2394–2397 (2010).
12. D. Knoll, S. Lischke, L. Zimmermann, A. Awny, M. Kroh, A. Peczek, K. Voigt, and K. Petermann, "Fabrication of high bit rate, monolithically integrated receivers in photonic BiCMOS technology," in *Group IV Photonics Conference (GFP)*, (IEEE, 2015), paper ThF5.

13. S. Lischke, D. Knoll, L. Zimmermann, A. Scheit, C. Mai, A. Trusch, K. Voigt, M. Kroh, R. Kurps, P. Ostrovskyy, Y. Yamamoto, F. Korndörfer, A. Peczek, G. Winzer, and B. Tillack, "High-speed, waveguide Ge p-i-n photodiodes for a photonic BiCMOS process," in *Bipolar/BiCMOS Circuits and Technology Meeting (BCTM)*, (IEEE, 2014), 29–32.
14. Y. Zhang, S. Yang, Y. Yang, M. Gould, N. Ophir, A. E. Lim, G.-Q. Lo, P. Magill, K. Bergman, T. Baehr-Jones, and M. Hochberg, "A high-responsivity photodetector absent metal-germanium direct contact," *Opt. Express* **22**(9), 11367–11375 (2014).

1. Introduction

Germanium (Ge) p-i-n photodiodes, coupled to a silicon waveguide, are the most widely used light detecting elements in technologies for Si-based photonic integrated circuits (PIC) or electronic photonic integrated circuits (ePIC). State-of-the-art waveguide-coupled Ge photodiodes typically provide an opto-electric, -3 dB bandwidth in the range of 25–45 GHz, a responsivity for the important 1.55 μm communication wavelength up to, but mostly lower than 1 A/W, and dark current densities (i_D) ranging from a few tens to several hundreds of mA/cm^2 , with all parameters mentioned here obtained at -1 V bias [1–5]. There are only few papers describing waveguide Ge photodiodes with bandwidths far beyond 50 GHz without making use of special effects like inductive gain peaking [6]. These works suggest that it is difficult to obtain simultaneously high bandwidth, high responsivity and low dark current: diodes with 60–90 GHz bandwidth, typically obtained at a bias between -2 V and -3 V, provide only a responsivity of 0.62 A/W [7], while even higher bandwidth values are accompanied by a very high dark current density (i_D) of 80 A/ cm^2 at -1 V [8].

In this paper, a novel waveguide-coupled Ge lateral p-i-n photodiode is demonstrated. The diode is foreseen to be an essential component of a recently introduced photonic BiCMOS process which monolithically combines state-of-the-art Si-photonics with high performance SiGe BiCMOS [9]. This new diode shows opto-electric, -3 dB bandwidths of 40 GHz at zero bias and more than 70 GHz at -1 V bias. Photodiode responsivity for 1.55 μm wavelength ranges from 0.84 A/W at zero bias to 1 A/W at -1 V, i.e. the diodes match or even surpass best responsivity values of the lower bandwidth diode generation. Measured room temperature dark current density is about 1 A/ cm^2 at -1 V bias, which does not significantly exceed the typical i_D range of diodes with much lower bandwidth. To our knowledge, such combined performance of Ge p-i-n photodiodes in terms of bandwidth, responsivity and dark current has never been shown before.

Our original photonic BiCMOS process includes a Ge lateral p-i-n photodiode, featuring a bandwidth of about 30 GHz (at -2 V) [9]. The diode is fabricated from a Ge layer selectively grown on top of a Si waveguide. Ge epitaxy is carried out after the BiCMOS baseline source-drain anneal step, which has a peak temperature of more than 1000 $^{\circ}\text{C}$, but before the BiCMOS CoSi_2 module. Thus, melting of the Ge layer and mixing it with underlying Si material is prevented on the one hand, and on the other hand, any risk of metal contamination of tools used for Ge epitaxy and pre-epitaxy wet cleaning is excluded. The B and P implantation steps applied for forming the p and n regions of the p-i-n diode are also carried out before silicide formation. To obtain a low-resistive CoSi_2 layer, as it is common in CMOS or BiCMOS processes, silicide process modules typically include two anneal steps with the second one featuring a temperature of 700 $^{\circ}\text{C}$ or even higher [10]. Under such anneal conditions an as-implanted P profile in Ge can significantly be broadened by diffusion [11]. In case of flattened doping profiles "slow" photo carrier diffusion can become a factor outweighing RC and high-field transit time that are usually considered diode bandwidth limiters. Fabrication of a diode with a target bandwidth of 50 GHz or more therefore becomes very challenging, in particular under the strict condition of changing not too much those baseline modules which are critical for BiCMOS device parameters [12].

Here, we will show that despite the processing restrictions of the BiCMOS environment outlined before, diodes can be fabricated showing simultaneously high bandwidth and high responsivity. Key for high responsivity is a new, low-loss contact scheme, which, moreover, also reduces the bandwidth-limiting effect of photo carrier diffusion.

2. Photodiode fabrication

Full photonic BiCMOS process flow including integration of a Ge photodetector module is described elsewhere [9]. Here, we focus only on the details of the detector module because the demonstrated measurement results stem from diodes fabricated in short flows where most BiCMOS frontend-of-line fabrication steps were cancelled, except the critical CoSi_2 module.

Diode fabrication flow is shown in Fig. 1. Together with Figs. 2 and 3 it explains also the essential diode structure features and the differences between former [9] and new devices.

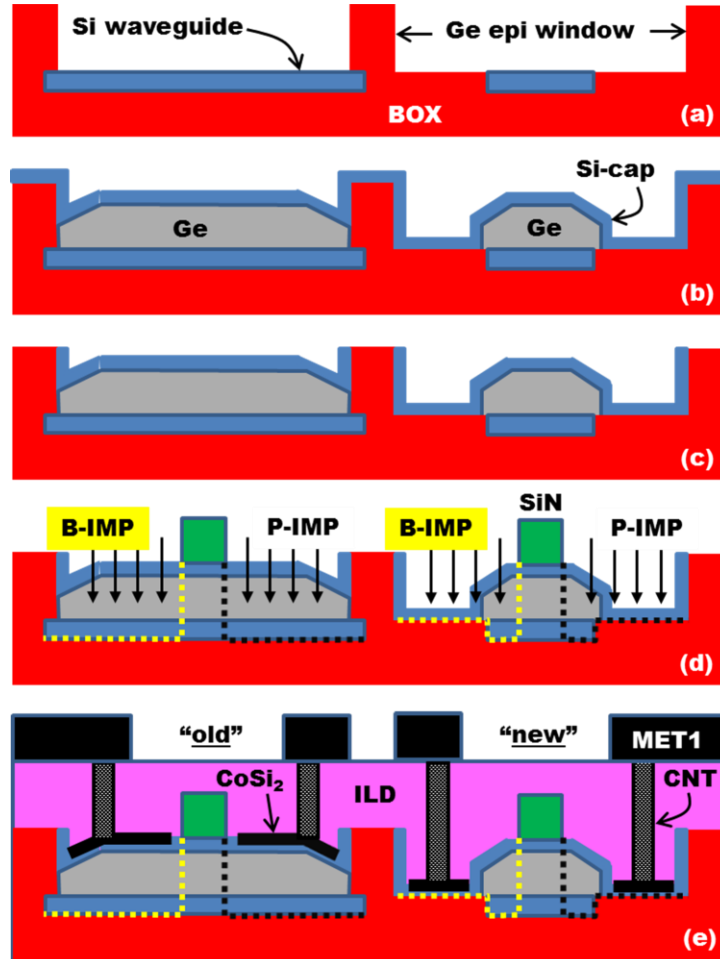


Fig. 1. Fabrication flow of Ge lateral p-i-n photodiodes with former layout (left → “old”) and new layout (right → “new”), illustrated by schematic cross sections perpendicular to the direction of light incidence: etching a window in an isolator layer stack with a planarized, some 100 nm thick silicon oxide layer on top (a); selective Ge epitaxy (about 400 nm) followed by non-selective Si deposition (b); silicon chemical mechanical polishing (Si-CMP) (c); formation of a 600 nm wide silicon nitride (SiN) pedestal followed by self-aligned implantation steps (d); CoSi_2 formation, contact (CNT) formation, first metal layer (MET1) deposition and structuring (e). BOX denotes the 2 μm thick buried SiO_2 layer beneath the 220nm thick Si waveguide.

Ge deposition was carried out at a temperature of 550 °C. To obtain low defect density, cyclic annealing was applied: annealing steps (at 800°C, 60 sec) were carried out after interrupting two times the deposition process and once again after completing the Ge growth. Implantation conditions for B and P were selected that provide nearly constant dopant concentrations (about $5 \times 10^{18} \text{ cm}^{-3}$ both for n- and p-side) through the Ge layer and the

underlying Si waveguide outside the regions which are protected by the SiN pedestal during implantation.

We emphasize that the new diode structure is the result of a layout variation only, as can easily be seen from Figs. 1–3, i.e. its fabrication does not need any process changes compared to the old device. We can therefore compare old and new devices fabricated on the same wafer, and measured even on the same dies, facilitating the understanding where particular performance improvements come from.

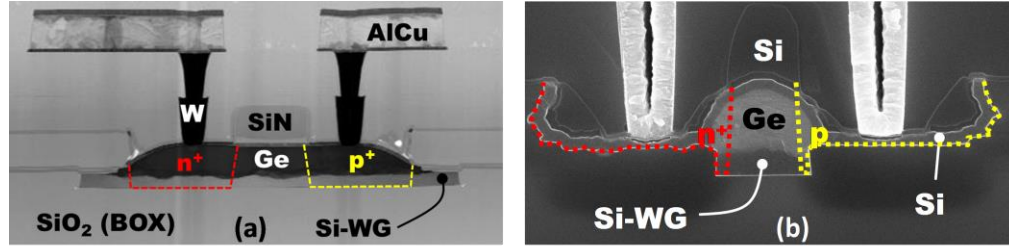


Fig. 2. Cross sections of Ge p-i-n photodiodes, perpendicular to the direction of light propagation: former layout (a) vs. new layout (b). For the new diode, a higher magnification was used for better detail resolution. Note that for diode fabrication the connection between AlCu lines and the CoSi₂ layer was at one point simplified here compared to the integrated module to save processing expense: Only one contact level was used instead the stacked, two levels of the BiCMOS integrated photodiode module as it is shown for the old diode.

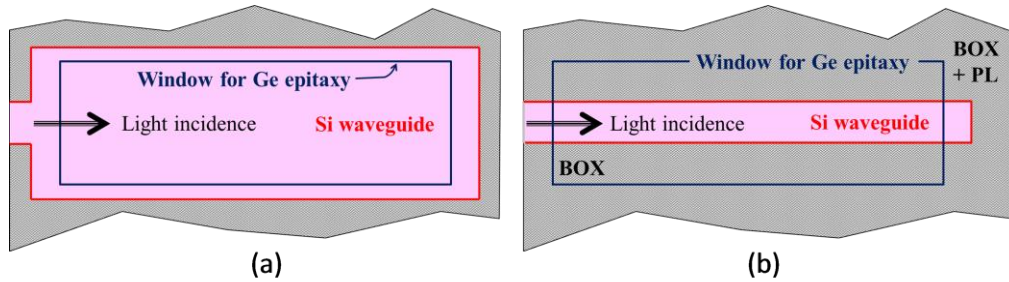


Fig. 3. Layout top view of old (a) and new diodes (b): Main difference is that, perpendicular to the direction of light incidence, the window for Ge epitaxy overlaps the underlying Si waveguide for the new diode, while it is inside the waveguide contour in the other case. PL denotes the isolator layer stack on top of BOX outside the epitaxy window. Width (3 μm) and length of epitaxy window (20 μm) are identical for new and old diodes. Width of Si waveguide inside the epitaxy window is 1 μm for the new diode.

There is an essential similarity as well as there are some differences between old and new devices. It is common to both diodes that Ge surfaces not covered by oxide are protected by a thin Si cap layer which has two advantages: It prevents Ge layer erosion during wet etch or cleaning steps applied in the PIC or ePIC fabrication flow after Ge growth. In addition, the Si cap allows for use of the BiCMOS CoSi₂ module for contacting the photodiode. Biggest difference is that the new diodes have lateral dimensions of doped Ge regions which are strongly reduced compared to the old diodes, i.e. the ratio of Ge i-layer width, which correlates to the width of SiN pedestal, to the lateral dimensions of doped Ge regions is much higher for the new devices. Another feature of the new diodes is that the tungsten contact plugs do not land on CoSi₂ layers formed directly over doped Ge regions, as it is the case for the old diodes, but laterally offset from Ge regions on doped Si offshoots, covered with CoSi₂.

Figure 4 shows different cases for the cobalt silicide formation on the new diode structure: Silicide is either formed on the silicon offshoot only, or it extends additionally on that Si layer part which covers laterally the Ge core. These different cases of silicide coverage can be obtained by careful control of an isolator (SiN) spacer formation process applied before cobalt deposition starts. Later we shall discuss consequences of this different CoSi₂ coverage.

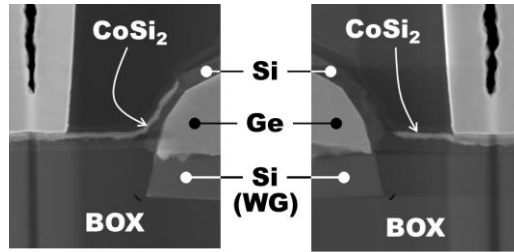


Fig. 4. TEM cross sections of different Ge p-i-n photodiodes with new layout: In one case, CoSi_2 is formed only on the horizontal silicon offshoots (right), while in another case the CoSi_2 layer extends additionally on that Si layer part which covers laterally the Ge core (left).

3. Experimental results and discussion

Figure 5 compares C-V and dark I-V curves of old and new Ge photodiodes with identical SiN pedestal width. Diodes were fabricated on the same wafer and measured on the same dies. Obviously, the new diodes show in tendency 10-20% higher capacitances compared to the simultaneously fabricated old diodes. Although the reason of this difference is not yet fully clear, we conclude from the C-V behavior that new and old diodes have similar doping profiles near the junctions which are not much affected by a reduction of doped Ge layer dimensions (new vs. old diodes). I-V curves, however, differ considerably between the diodes: First, we see a stronger resistive forward current limitation for the new diodes which is not surprising considering the changed contact scheme. Second, we observe a nearly by a factor of 3 increased forward current at low bias for the new diodes which suggests that the new diode structure leads to lower minority carrier diffusion length compared to the old one (at this point one cannot decide whether the changed characteristics are due to electrons or holes or due to both carriers). Third, show the new diodes a higher dark current at reverse bias. The around 100 nA measured at -1 V bias for the new diodes correspond to a current density of 1 A/cm^2 .

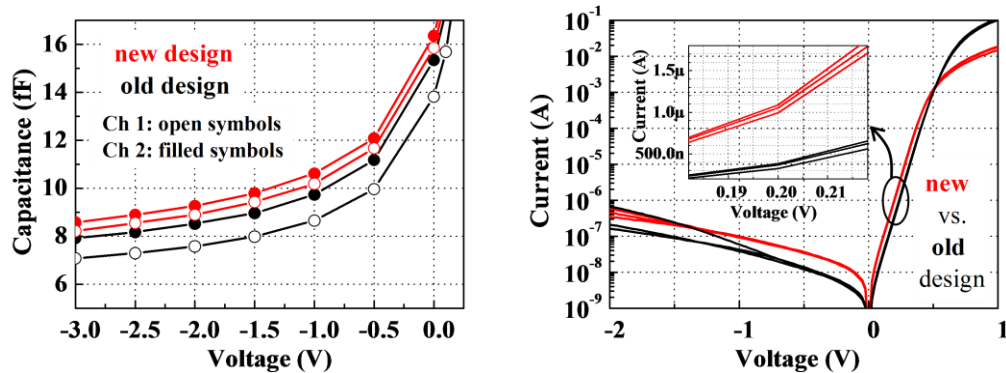


Fig. 5. Electrical characteristics of Ge p-i-n photodiodes with old and new design (low CoSi_2 coverage): Capacitance vs. voltage curves are shown on the left. C values were extracted from small-signal parameter measurements under use of open- and short-structure de-embedding of supply lines and bondpads. Diodes were measured on 2 dies (Ch1, Ch2). DC characteristics of non-illuminated diodes are shown on the right. Junction area of both diodes is about $10 \mu\text{m}^2$. Diodes were measured here on 3 dies.

Normalized response (s_{21}) versus frequency curves, measured between zero and -2 V bias are shown in Fig. 6, on the left. One can immediately see that the new diodes provide much higher bandwidths compared to the old ones. The -3 dB bandwidth at zero bias is at least 40 GHz but, already at -1 V, it cannot be determined properly anymore because we exceed the upper frequency limit (67GHz) of the measurement system. Here, we do not provide bandwidth values obtained by extrapolation of available measurement data beyond 67 GHz. How-

ever, we think it is safe to say that it is at least 70 GHz. Figure 6 proves also that these very high bandwidth values can be reached in a stable manner. It shows, on the right, wafer distribution and histogram of -3 dB bandwidth values, estimated for new diodes directly from the response vs. frequency curves measured at zero bias. Note that diodes on all 61 dies of a 200 mm diameter wafer were measured, without a single device failing. Mean value here is 42.3 GHz with a very low sigma of 2.1 GHz demonstrating good manufacturability of the new diodes.

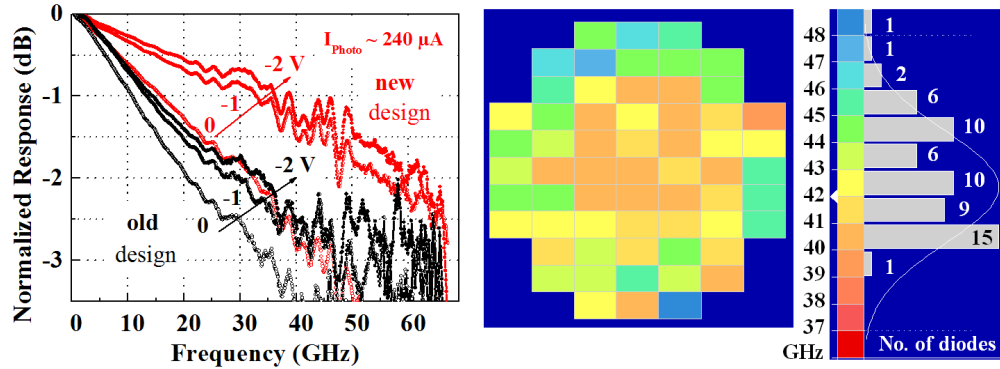


Fig. 6. Opto-electric high frequency behaviour of Ge p-i-n photodiodes with old or new design (low CoSi₂ coverage): On the left, normalized response vs. frequency curves, measured at different bias, are shown for old and new diodes. The devices were fabricated on the same wafer and measured on the same die. A commercial Agilent 67 GHz lightwave component analyzer was used for characterization. On the right, a wafer distribution and histogram of -3 dB bandwidth values of new diodes is shown. Bandwidth values were estimated here from response vs. frequency curves measured at zero bias (61 diodes were measured).

An interesting question is where does the strong bandwidth improvement of the new diodes come from? Obviously, the improvement was reached despite of similar (even a bit higher) capacitances and significantly higher series resistances (see diode forward current behavior in Fig. 5), compared to the old devices. This implies that the improvement cannot result from a reduced charging time (RC) effect. We can also exclude a high-field transit time effect because the capacitance curves in Fig. 5 do not point to strongly differing depletion widths of both diodes. The observed bias behavior (higher bandwidth with increased reverse bias) indicates as well that the bandwidth behavior (of both diodes) is not limited by transit times. An additional, but often neglected effect which can limit the bandwidth of photodiodes is photo carrier diffusion [13]. Assuming that diffusion is the bandwidth-limiting effect for the diodes under investigation and that the new diode structure leads to reduced diffusion length would qualitatively explain the improvement. The forward current behavior shown in the insertion of Fig. 5 also supports this assumption, in our opinion. Moreover, the observed bias dependence of response vs. frequency curves does not contradict this assumption. The question remaining is in which way the new diode structure reduces diffusion length? Depletion width of both diodes, as calculated from the capacitance values of Fig. 5, is at most 200 nm at -2 V which is much lower than the width of the SiN pedestal (600 nm). This means that for both diodes only a narrow Ge region beneath the SiN layer stripe includes an electrical field, while optical field extends certainly also to Ge regions which are not depleted, i.e. do not have electrical field. Because the lateral dimensions of non-depleted Ge regions are much lower for the new diodes it implies that a reduction of diffusion length “by design” is the main factor responsible for the strong gain in bandwidth. However, one cannot exclude on base of the available measuring data that a defect-related effect contributes in addition to the diffusion length reduction. That the new diodes are more defective is suggested by the higher reverse bias currents which can be seen from Fig. 5.

All results, shown so far for diodes with new design stem from devices for which the CoSi₂ contact layer was formed as depicted in Fig. 4, right. Figure 7 illustrates that a higher

CoSi₂ layer coverage, as illustrated in Fig. 4 left, lowers the series resistance approaching the behavior of the old diodes in this respect. However, we did not find a significant effect of the lower resistance on the response vs. frequency behavior of the new diodes which we see as another indication that our assumption regarding the bandwidth-limiting effect is correct.

Next, we focus on the photocurrent behavior of the different diodes. Figure 8 shows photocurrent vs. laser power curves for new diodes with low CoSi₂ coverage, measured under different bias conditions. From these curves and considering that the lowest loss value of the used grating couplers was, for 1.55 μm wavelength, -2.7 dB, worst case values for the internal diode responsivity were estimated. Table 1 summarizes the values and compares these with the responsivities of the other diodes. Note that for responsivity estimation of the new diodes linear data fitting was applied which did, however, not include the photocurrents obtained at highest laser power (9.8 mW), where a certain saturation effect can be observed, in particular for the zero bias case.

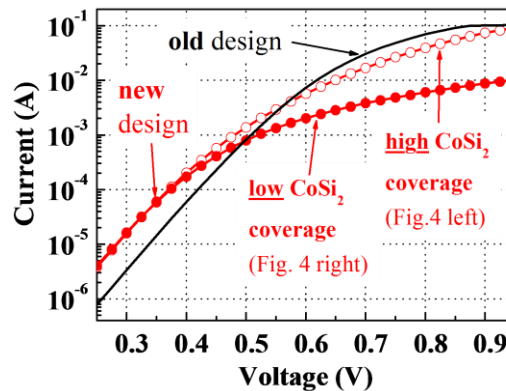


Fig. 7. Forward I-V characteristics of old and new Ge photodiodes. Two variants of new diodes, differing in the CoSi₂ coverage, were measured.

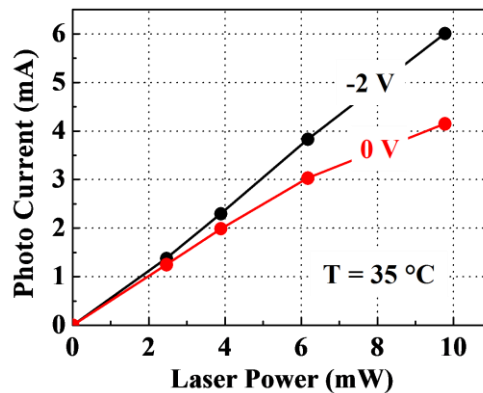


Fig. 8. Photocurrent vs. CW laser power at the fiber end for Ge photodiodes with new design and low CoSi₂ coverage, measured for 0 V and -2 V bias.

Table 1. Internal responsivities (R_{int}) at 1.55 μm wavelength for the diodes under investigation

Diode type	new			old
CoSi ₂ coverage	low	high		
Bias (V)	0	□1	□2	□2
R _{int} (A/W)	0.84	1.00	1.06	0.64
				0.25

Several effects can be seen or concluded from Table 1: The new diode design provides strongly improved internal responsivity compared to the old design, confirming recently published results regarding the role of metal-germanium direct contact on responsivity [14]. The new diode with low CoSi₂ coverage shows at 1.55 μm wavelength responsivities in the range of 0.84-1.06 A/W between zero and -2 V bias, a performance not yet published so far for germanium p-i-n photodiodes with far more than 50 GHz bandwidth. Considering all results (new vs. old design, low vs. high CoSi₂ coverage) it is suggested that the full responsivity gain results from preventing both free carrier and metal absorption.

4. Summary

In summary, we have demonstrated for the first time a Ge p-i-n photodiode which provides more than 70 GHz bandwidth, together with an internal responsivity of more than 1 A/W for 1.55 μm wavelength, at a medium level of reverse bias dark current. There are several indications that the strong gain in bandwidth performance results from a photo carrier diffusion length reduction, while high responsivity is reached by a novel low-loss contact scheme.

Acknowledgments

We gratefully acknowledge partial support by German Ministry of Research and Education (BMBF), projects SASER (grant 01BT1209), MOSAIC (grant 13N12434), and RF2THzSiSoC (grant 16BP12503), by German Research Foundation (DFG) in the framework of the Sonderforschungsbereich SFB787, and by EU-FP7 project BEACON (grant 607401).